NASA Technical Memorandum 103103

The Vibro-Acoustic Mapping of Low Gravity Trajectories on a Learjet Aircraft

C.M. Grodsinsky and T.J. Sutliff
Lewis Research Center
Cleveland, Ohio

Prepared for the
Second Workshop on Microgravity Experimentation
sponsored by the National Research Council of Canada
Ottawa, Ontario, Canada, May 8–9, 1990

NASA

THE VIBRO–ACOUSTIC MAPPING OF LOW GRAVITY TRAJECTORIES ON A LEARJET AIRCRAFT

C. M. Grodsinsky and T. J. Sutliff

NASA Lewis Research Center
Cleveland, Ohio 44135

Abstract

Terrestrial low gravity research techniques have been employed to gain a more thorough understanding of basic science and technology concepts. One technique frequently used involves flying parabolic trajectories aboard the NASA Lewis Research Center Learjet aircraft. A measurement program was developed to support an isolation system conceptual design. This program primarily was intended to measure time correlated high frequency accelerations (upto 100 Hz) present at various locations throughout the Learjet during a series of trajectories and flights. As suspected, the measurements obtained revealed that the environment aboard such an aircraft can not simply be described in terms of the static level low gravity "g vector" obtained, but that it also must account for both rigid body and high frequency vibro–acoustic dynamics.

Nomenclature

e_r = body fixed radial direction
e_t = body fixed tangential direction
EU = engineering units
g = non–dimensional acceleration ($m/s^2/g_o$)
g_o = acceleration of gravity (9.81 m/s^2)
i = horizontal inertial unit vector direction
j = vertical inertial unit vector direction
r = vector from inertial ref. to reference sensor
$\dot{r}$ = time derivitive of r
$\ddot{r}$ = time derivitive of $\dot{r}$
r_t = vector from inertial ref. to body fixed accel.
$\dot{r}_t$ = time derivitive of r_t
$\ddot{r}_t$ = time derivitive of $\dot{r}_t$
t = distance from the reference sensor to body fixed tangential location
v = velocity of aircraft
$\dot{v}$ = time derivitive of v
x = horizontal aircraft coordinate system
X = horizontal inertial coordinate system
y = out–of–plane aircraft coordinate system
Y = vertical inertial coordiante system
z = vertical aircraft coordinate system
ξ = angular rotation of aircraft referenced to X
$\dot{\xi}$ = time derivitive of ξ
$\ddot{\xi}$ = time derivitive of $\dot{\xi}$
τ = time

Introduction

From the beginning of the space program, man has been intrigued by the phenomenon of weightlessness. Development of more accurate theories for physical and chemical laws have been possible through the study of experimental results when the effects of gravity can be substantially reduced or eliminated. The ultimate environment for weightless research one day will be within the orbiting Space Station Freedom. However, for many scientific applications, earthbound methods are being employed to simulate the idealized condition of weightlessness for the benifit of improving upon current theories.

A variety of tools are available to provide weightless conditions for basic materials research. Numerous freefall methods have been developed to provide short duration periods of near–weightlessness, or "microgravity". Drop tubes and towers have produced "microgravity" durations of one to five seconds. Aircraft flying parabolic trajectories have generated periods of low gravity for about 15 seconds. Sounding rockets and, of course, on–orbit launch vehicles have also been used. Each technique has benefit and liability tradeoffs associated with it

such as available test duration versus cost per test. Also, all techniques have specific limitations on the degree of ideal weightlessness which they provide.

Limited low to moderate frequency measurements have been acquired to quanitify the low gravity environment generated by "microgravity" techniques. The actual environment for an aircraft flying research trajectories is quite dynamic, both mechanically and acoustically. In order to derive full benefit from data obtained when experiments are conducted aboard these aircraft, it is not only required to understand the low to moderate frequency accelerations present but also necessary to characterize the broadband aircraft vibro–acoustic environment. In addition, typical low frequency data have been measured at the reference sensors, from which the pilots control the trajectory path. These sensors have implemented lowpass filters to aid the pilot in his ability to manually control the parabolic trajectory. The upper cutoff frequency of these filters have been chosen to be on the order of 2 Hz. Some data does exist from sensors located at the experiment location; however, this single point information was lowpass filtered similar to the control sensors, and was typically not time correlated to the reference sensor accelerations.

High frequency vibro–acoustic information and simultaneously acquired multiple point low frequency information regarding rigid body motion have not previously been acquired in any tangible form. Both phenomena may be responsible for inconclusive "microgravity" research results obtained aboard aircraft flying parabolic trajectories because information regarding the true induced environment may have been overlooked. This paper presents a summary of results obtained from a vibro–acoustic measurement program conducted during a series of low gravity trajectories flown on the NASA Lewis Research Center Learjet. The specific data summarized in this paper will encompass the simultaneously acquired multipoint acceleration information obtained from a total of 25 trajectories conducted over five seperate flights.

A measurement program was conceived which involved instrumenting the fuselage and an experiment rack used in supporting typical low gravity experiments in the Learjet with 13 channels of accelerometers and three channels of pressure transducers. The locations of these various sensors were determined in order to build a time history of the dynamics involved in the flight of such a parabolic trajectory and thus determine the typical rigid body and vibro–acoustic loading a payload would experience.

By characterizing the low gravity environment obtainable on the Learjet one can make conclusions as how to design an isolation system to absorb the disturbances encountered using passive means, or to actively control the environment an experiment would experience during these trajectories.

Scope of Data Acquisition

In characterizing these series of parabolic trajectories for the design and development of an isolation system, one is primarily concerned with the magnitudes and frequency spectrum of vibratory energy within which such a system would be active. The constant loading or residual static acceleration a package experiences is important; however, in terms of isolation one need only know the magnitude of support needed for such a package.

In the process of performing this characterization one can get a fairly accurate account of the rigid body dynamics of a package in the Learjet due to its position relative to the electronic center–of–gravity. This electronic center–of–gravity arises since the system by which the pilots fly the parabolic trajectory is an electronic inertial reference sensor.

Theoretical Control of a Ballistic Trajectory

The system by which these trajectories are flown may best be described by theoretically deriving the equation of motion for the parabolic flight trajectory in two dimensions, or assuming simple planer motion. The typical ballistic trajectory is illustrated in Figure 1 where the low gravity portion of this trajectory begins after the high g maneuver as indicated in the figure. The coordinates for the trajectory and body fixed axes will be defined as shown in

Figure 2.

Referencing Figure 2, the vector r is defined as the vector tracking the position of the trajectory reference sensor to the inertial coordinate system. In the body fixed frame the distance from an accelerometer to this coordinate system is defined by a vector length t in the e_t direction. In defining the trajectory as previously stated the velocity of the reference sensor can be written in the inertial coordinate system as follows:

$$(1) \qquad \dot{r} = (v\cos\xi)i + (v\sin\xi - g_o\tau)j$$

and the velocity of the characterization sensor location is

$$(2) \qquad \dot{r}_t = (v\cos\xi + t\dot{\xi}\sin\xi)i + (v\sin\xi - g_o\tau - t\dot{\xi}\cos\xi)j.$$

In order to obtain the accelerations experienced by the two points one must take the derivative of these vectors with respect to time. By doing so the acceleration of each point in the inertial frame become:

$$(3) \qquad \ddot{r} = (\dot{v}\cos\xi - v\dot{\xi}\sin\xi)i + (\dot{v}\sin\xi + v\dot{\xi}\cos\xi - g_o)j$$

and

$$(4) \quad \ddot{r}_t = (\dot{v}\cos\xi - v\dot{\xi}\sin\xi + t\dot{\xi}\sin\xi + t\dot{\xi}^2\cos\xi)i + (\dot{v}\sin\xi + v\dot{\xi}\cos\xi - t\dot{\xi}\cos\xi + t\dot{\xi}^2\sin\xi - g_o)j.$$

To establish a convenient reference to correlate actual experimental acceleration data, these accelerations will be written in the body fixed coordinate system. Thus, by using the appropriate transformation the two acceleration equations in the body fixed frame become:

$$(5) \quad \ddot{r} = (v\dot{\xi}^2 - g_o\cos\xi)e_r + (\dot{v} - g_o\sin\xi)e_t$$

and,

$$(6) \qquad \ddot{r}_t = (v\dot{\xi}^2 - t\ddot{\xi} - g_o\cos\xi)e_r + (\dot{v} - t\dot{\xi}^2 - g_o\sin\xi)e_t.$$

The rotational velocity and forward thrust of the aircraft is being controlled in order to cancel the acceleration due to gravity in the body fixed axes. This control is accomplished by viewing a light emitting diode (LED) display where one axis of the display is proportional to acceleration in the radial direction and the other axis is proportional to tangential acceleration. Both of these accelerations are measured at the remotely mounted reference sensor.[1] The control–loop is closed by the pilots controlling the pitch rate and thrust of the aircraft.

By controlling the aircraft trajectory in this manner, the reference sensor, in effect, becomes the electronic center–of–gravity of the aircraft. As seen in equation (4) there is an additional acceleration term due to the pitch rate and the pitch rate as a function of time in the radial and tangential coordinate directions, respectively. These acceleration components are linearly related to the distance from a point to the electronic center–of–gravity. This theoretical development shows that the residual acceleration of an experiment can be substantially different from that of the control sensor.

Test Setup and Definition

Implementation of a measurement program aboard the Learjet 25 aircraft involved installation of a series of accelerometers and microphones as well as a portable data acquisition system. The accelerometers were located along the aircraft seat rails and at the base of a typical experiment rack. This rack also contained the signal conditioning hardware. The microphones were located behind the pilot, on the signal conditioning rack, and behind the rear bench seat. The acquisition system was located within an adjacent experiment rack.

Each acceleration measurement channel consisted of an equivilent four arm piezoresisitive accelerometer (Endevco model 2262–25) wired to a strain gage bridge amplifier (Vishay model BA–4). Prior to installation into the Learjet, these transducer–amplifier pairs were adjusted and balanced to provide a known full scale voltage reading in a 1 g field, and a zero (null) reading when positioned horizontally to this field.

Three condenser microphone (pressure) transducers (Bruel & Kjaer model 4130) were similarly integrated together with their preamplifiers and power supplies. A calibration pistonphone was used to adjust and set the desired full scale voltage for each channel to a known sound pressure level.

Each of the 16 measurement channels, in turn, was then integrated into the rack or into its appropriate aircraft measurement position. The specific measurement locations within the Learjet 25 are shown in Figure 3. The output of the thirteen BA–4 amplifiers and three B&K power supplies were routed to a 16 channel high–speed digital data acquisition system (Gen Rad model 2515) in an adjacent rack. This system has the ability to simultaneously acquire and store 16 channels of contiguous time data at a throughput rate of 512 samples/ sec/ channel. Since the system is a 12 bit system, the data resolution capability is one part in 4096, based on the full scale voltage set for each channel. Built–in anti–aliasing filters were automatically set to 160 Hz for the usable frequency range of 0–128 Hz. Appropriate full scale voltage ranges for each channel were set, and calibration values to convert the data to appropriately scaled engineering units (g or Pa) were entered into a data acquisition condition table. These conditions, including full scale ranges, are summarized in Table 1.

Program files were created to automate the command entries necessary to acquire data while in the air. Required user actions prior to trajectory entry was to select the trajectory number next being flown, and to begin acquistion/ data storage as the entry maneuver was initiated.

Data Acquisition

A typical data gathering flight began with a minimum of a 30 minute equipment warmup following engine start. During flight to the test area, the appropriate pre–programmed automated data acquisition files were recalled and checked for accuracy. Some basic data checks were conducted to see that response from each channel was present.

Once the flight crew was satisfied that smooth air had been found for the flight test altitude range, the first of upto six "microgravity" trajectories per flight were initiated. For each trajectory flown, data storage was initiated prior to the 2.5 g pullup maneuver. Acquisition duration for all trajectories was 56 seconds. This duration would insure recording of the entire "microgravity" period, including the entry and exit maneuver characteristics. Following two flight days from which preliminary data was acquired, a total of 24 "microgravity" trajectories over five additional flight days were acquired. In addition, for data checking purposes, a single straight and level (1 g) data file was gathered at the mid–point of the flight matrix. Following each flight, data was transferred from the Gen Rad 2515 to a mainframe VAX computer where the data was analyzed.

Upon test sequence completion, the data gathering equipment was removed from the Learjet. The measurement transducer systems underwent a post flight calibration check similar to that used for preflight balancing and ranging. Zero–shifts were detected and noted for all thirteen accelerometer channels. The typical equivilent g shift present was on the order of 0.01–0.06 g's, with one channel being shifted as far as 0.26 g's, see Table 2. It was found that, once corrected for this DC offset, the full scale (1 g) voltages were within 1% of the previously set values. The microphone calibration values were within 0.2% of their pre–flight values and have no DC component.

Experimental Results

Rigid Body Dynamics

The rigid body dynamics, defined in the theoretical formulation as a three degree–of–freedom problem, can be compared with the actual rigid body motion of the aircraft by digitally filtering the acceleration data, and plotting the low frequency rigid body dynamics of the flight.

In order to attempt a correlation of the low frequency residual accelerations with the theoretical planer equation of motion, one must have an accurate measure of the electrical bias inherent in any data acquisition system. If the offsets were not corrected and the bias voltages were constant for each data channel the relative

rigid body acceleration from point to point would give the applicable rigid body correlation. This assumes no out–of–plane dynamics are present. However, in the test setup used this was not the case and therefore, a correction was required in order to attempt a quantitative measurement of the residual acceleration due to the angular acceleration of the aircraft. Thus, in an attempt to quantify the residual offset expected a block of straight and level acceleration data was taken in order to obtain a relative offset correction. All the tangential acceleration channels were then referenced to one location. In addition to this straight and level correction approach the system was put through a post calibration to determine offsets. This bias offset correction data was then compared with the offset corrections found from the straight and level data. Both offset correction factors are shown in Table 2.

As shown by the two offset correction approaches, their are large discrepencies between these correction approaches. However, the residual accleration trends for locations 6, 7, and 8z+, after being corrected by both offset approaches, did show the same trends predicted by equation (6) for the planer motion of the aircraft. In order to check the validity of these trends the ratio of relative DC accelerations between these three points must be constant over a flight, demonstrating the electrical offsets were not drifting during a flight. Table 3 shows these ratios for flight seven. The discrepencies in these calculations most likely occur because the three acceleration measurement locations are not exactly in the same vertical plane as the reference sensor and thus, out–of–plane dynamics are entering into the calculations. The attempt at an accurate calculation of the angular acceleration was not possible with this data. However, in a follow on project, a new data acquisition system accurately measuring electrical offsets will be flown. A gyroscope will also be included for the verification of the calculated angular accelerations irrespective of out–of–plane accelerations. Although, the calculated angular accelerations lack in accuracy they are listed, for a number of the flights, in Table 4 giving statistical support to the consistency of the rigid body response of the aircraft.

Figure 4 shows a typical residual acceleration trend for locations 6, 7, and 8z+. The curves demonstrate the offset trends due to the angular acceleration of the aircraft. These trends are consistant from flight to flight and trajectory to trajectory. The oscillatory accelerations superimposed on the residual time trace show the pilots attempting to maneuver the aircraft to control the angular velocity. This acceleration has about a 2–2.5 Hz frequency with variying magnitude, dependent on the pilot and flight conditions.

High Frequency Dynamics

The inherent problems previously discussed with the zero–point drift of the bridge amplifiers, fortunately has no bearing upon data reduced for high frequency purposes. The high frequency data analysis involved determining only the dynamic response characteristics present due to the airframe, the acoustic environment, and the experiment mounting rack. As such, any DC shift present does not affect the dynamic data reduction process.

The primary high frequency data reduction technique utilized and discussed here is the calculation of an autospectrum for each channel during its "microgravity" period. These autospectra are presented as power spectral density (PSD) amplitudes in EU^2/Hz versus frequency in Hz. The simultaneous sample–and–hold capability of the Gen Rad 2515 also provides the ability to not only calculate single channel autospectra PSD's, but also to employ cross spectral analysis techniques. With such methods, channel to channel phase information may be extracted as well. Although this cross channel information is available, it will not be presented at this time.

The methodology employed to determine the power spectral densities (PSD's) for each accelerometer and microphone during the "microgravity" period first involved determining the times at which the low g period began and ended (same value for all data from a single trajectory), determining how many ensembles (time samples) could be processed into a spectrum average for that duration, and then processing the autospectra and cross spectra PSD's. Typically, there was enough "microgravity" duration to obtain an average of

six to eight ensembles of processed time data. A basic check of random process stationarity was conducted. It was demonstrated that there was minimal variation of the resultant PSD's if five or more "microgravity" ensembles were used. It was also noted that there was significant variation in the PSD's if the entire 56 seconds of data were processed as a set of ensembles. This demonstrated the non–stationarity of the entry/ "microgravity"/ exit high frequency time domain process. An example of a pitch (z–axis) accelerometer time domain high frequency response can be seen in Figure 5. It clearly shows the drop in response level occurring during the "microgravity" period compared to the entry and exit maneuvers.

It is also obvious from typical time traces that the dynamic response peak acceleration levels seen in the microgravity period do exceed the desired quasi–static acceleration environment, sometimes by an order of magnitude. In the case of the T–rail mounted accelerometers, the vertical peak dynamic acceleration is on the order of 0.10 g–pk. The rack accelerometer data indicate the presence of some natural structural isolation, as they are on the order of 0.03 to 0.08 g–pk regardless of measurement direction. (A strip chart representation of accelerometers 8z, 1x, 1y, and 1z are shown in Figure 6.) Although the rack offers some attenuation at the base, these levels are still higher than the quasi–static levels of 0.02 g thought to be readily achievable.

As mentioned earlier, the flight–to–flight variation in low frequency and DC levels measured during the "microgravity" period of a trajectory was small. Inconsistencies in the flight regime and flight conditions such as aircraft weight causing differing structural responses, the altitude effects on engine output performance (RPM variations), and even the variability on the entry technique levels and styles from pilot to pilot will tend to affect the high frequency vibro–acoustic response of the aircraft. Even so, the individual channel responses still demonstrated a degree of consistency from one trajectory to the next.

More substantially, spacial variations were detected between the measurement locations acquired. For example, the accelerometers mounted vertically, directly to the T–slots, demonstrated responses fairly broadband in nature, while those accelerometers vertically attached to the lower portion of the experiment rack indicated modal response (resonance) characteristics. Similarly, the rack horizontal measurements show significant resonances at a number of frequencies. An example of these characteristics are shown in Figure 7. PSD's for an accelerometer on the T–slot at 7z, and on the rack for location 1x, 1y, and 1z for the same flight are shown. A microphone PSD for location 11 is also included. Table 5 presents typical peak frequencies observed throughout the flight matrix for the three rack mounted accelerometers at location 1.

Based on the dynamic results seen, there appears to be merit in attempting to isolate the high frequency vibro–acoustic inputs to which experiments are being subjected. The results in Table 5 show the lowest requiring isolation is on the order of 20 Hz. To be useful, it appears that an isolation frequency of 5 Hz and below would significantly improve the "ride".

Conclusions

"Microgravity" vibro–acoustic information was acquired on a series of parabolic trajectories flown aboard a NASA Learjet 25 research aircraft. These data update previously acquired information regarding the low frequency acceleration environment of typical trajectories. They also provide an insight to the high frequency dynamics present during the "microgravity" research experimentation period.

The low frequency experimental data also indicated apparent trends of rigid body dynamics being present during trajectories. A theoretical model for these rigid body dynamics was developed. This model was able to substantiate the presence of an unaccounted–for rigid body angular acceleration about the flight control accelerometer.

The reduced data aid in quantifying the true environment present at an experimentation location. The low frequency information gathered may lead to an improvement of the flight trajectory control at the experiment location, while the high frequency information obtained may lead to the implementation of an isolation system for selected experiments

sensitive to dynamic inputs.

Continued work is in progress to develop and fly both passive and active isolation systems. In addition, the flight data gathering system is planned to include more accurate acceleration instrumentation, a higher degree of resolution, and a gyroscope, from which direct angular acceleration measurements may be made.

References

1. Marc G. Millis, Acceleration Display System for Aircraft Zero–Gravity Research, NASA TM–87358, 1987.

2. Users Guide to Learjet for Low–Gravity Research

3. Structural Dynamics Research Corp., Reference Manual for Modal–Plus 9.0, 1985

TABLE 1 - DATA ACQUISITION CHANNEL SETTINGS

DATA CHANNEL	DIRECTION	SENSOR LOCATION	FULL SCALE RANGE
1	2 Z+	2	4.0 g.
2	6 Z+	6	5.0 g.
3	7 Z+	7	4.0 g.
4	8 Z+	8	5.0 g.
5	4 Z+	4	5.0 g.
6	4 X-	4	4.0 g.
7	3 Y-	3	5.0 g.
8	3 Z+	3	5.0 g.
9	1 X-	1	5.0 g.
10	1 Y+	1	4.0 g.
11	1 Z+	1	4.0 g.
12	5 Y+	5	4.0 g.
13	5 X+	5	5.0 g.
14	9 Z+	9	15.85 Pa.
15	10 Z+	10	15.85 Pa.
16	11 Z+	11	15.85 Pa.

TABLE 2 - OFFSET CORRECTIONS

SENSOR LOCATION AND DIRECTION	STRAIGHT AND LEVEL CORRECTION (1)	ZERO OFFSET CORRECTION (2)
1 Z+	+0.0230	+0.0020
2 Z+	+0.0014	+0.0132
3 Z+	-0.2261	-0.2866
4 Z+	+0.0063	+0.0088
6 Z+	+0.1114	-0.0195
7 Z+	+0.0568	+0.0044
8 Z+	0.0	+0.0231
1 X-	(NOT APPLICABLE)	+0.0129
1 Y+	" "	+0.0440
3 Y+	" "	-0.0178
4 X-	" "	+0.0640
5 Y+	" "	-0.0245
5 X+	" "	-0.0125

(1) Based on flight data at constant airspeed/wings level conditions; corrected for zero at 8 Z+

(2) Based on post flight calibration readings

TABLE 3 - SINGLE FLIGHT COMPARISON OF MEASURED (UNCORRECTED) ACCELERATION RATIOS NORMALIZED TO 8Z+ (1)

TRAJECTORY	MEASURED $\left(\frac{8Z}{7Z} \cdot \frac{8Z}{6Z}\right)$	ERROR (IDEAL - MEASURED)
1	0.59348	0.01235
2	0.55960	0.04623
3	0.48830	0.11753
4	0.49087	0.11496
5	0.50065	0.10518
6	0.52088	0.08495
MEAN	0.52563	0.08020
STANDARD DEVIATION		0.04244

(1) Ideal distance ratio = 0.60584

TABLE 4 - CALCULATED ANGULAR ACCELERATION
(ASSUMED PLANAR MOTION OF LOCATIONS 6, 7, 8)

A. BIAS CORRECTED DATA

FLIGHT: TRAJECTORY	RESIDUAL ACCELERATION (8Z-7Z)	(8Z-6Z)	CALCULATED (1) ROTATIONAL ACCELERATION (RAD/S^2) (8Z-7Z)	(8Z-6Z)
3:1	0.124	0.176	1.15919	0.99199
3:2	0.108	0.179	1.01034	1.01059
3:3	0.0851	0.153	0.79171	0.86630
4:1	0.170	0.272	1.58494	1.53533
4:2	0.159	0.271	1.48667	1.52857
4:5	0.128	0.230	1.19082	1.29635
5:1	0.0975	0.186	0.90707	1.04830
5:2	0.0910	0.183	0.85218	1.03480
6:1	0.128	0.206	1.19082	1.16108
7:1	0.122	0.217	1.13965	1.22590
7:2	0.116	0.216	1.08383	1.22026
7:3	0.0980	0.205	0.91172	1.15544
7:4	0.0940	0.196	0.87451	1.10472
7:5	0.0950	0.195	0.88381	1.09908
7:6	0.0960	0.191	0.89312	1.07653

B. STRAIGHT AND LEVEL CORRECTED DATA

FLIGHT: TRAJECTORY	RESIDUAL ACCELERATION (8Z-7Z)	(8Z-6Z)	CALCULATED (1) ROTATIONAL ACCELERATION (RAD/S^2) (8Z-7Z)	(8Z-6Z)
4:2	0.085	0.118	0.79080	0.66509
5:2	0.017	0.030	0.15815	0.16907
5:3	0.010	0.012	0.09331	0.07062
6:2	0.047	0.052	0.43727	0.29309
7:1	0.046	0.062	0.42795	0.34945
7:2	0.040	0.061	0.34758	0.34607
7:3	0.022	0.050	0.20939	0.28523
7:4	0.019	0.041	0.17676	0.23390
7:5	0.019	0.035	0.18234	0.20065
7:6	0.018	0.035	0.17304	0.19727

(1) Distance from 8 to 7 is 41.5 in.
Distance from 8 to 6 is 68.5 in.

TABLE 5 - FLIGHT-TO-FLIGHT VARIATION IN FREQUENCY RESPONSE FOR RACK LOCATION 1

FLIGHT: TRAJECTORY	RESPONSE DIRECTION	PEAK FREQUENCIES (HZ) (LOW) → (HIGH)
3:2	X	21 24 42 110
	Y	24 42 110
	Z	21 29 42
4:4	X	14 20 24 40 80 112
	Y	25 40 80 112
	Z	22 40
5:2	X	20 26 77 109
	Y	26 43 109
	Z	22 32 42
6:1	X	21 110
	Y	20 25 40 90 110
	Z	22 40
6:5 (STRAIGHT & LEVEL)	X	95 110
	Y	12 24 26 34 40-48 68 95 110
	Z	20 24 30 45-48 68 95 110

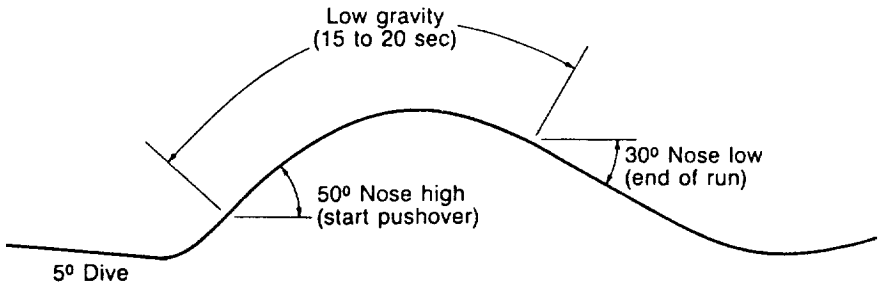

Altitude, ft:	~11 000	~18 000	~11 000
Indicated airspeed, knots:	360	180 to 220	----------
Gravity, g:	2 to 2-1/2 (pullup)	Low	2 to 2-1/2 (pullup)

FIGURE 1

Typical Aircraft Ballistic Trajectory

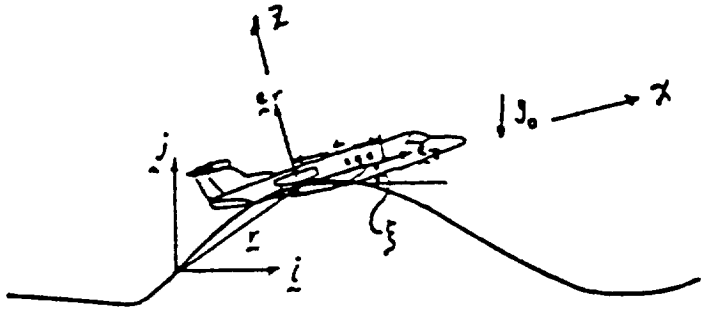

FIGURE 2
Coordinate Systems Definitions

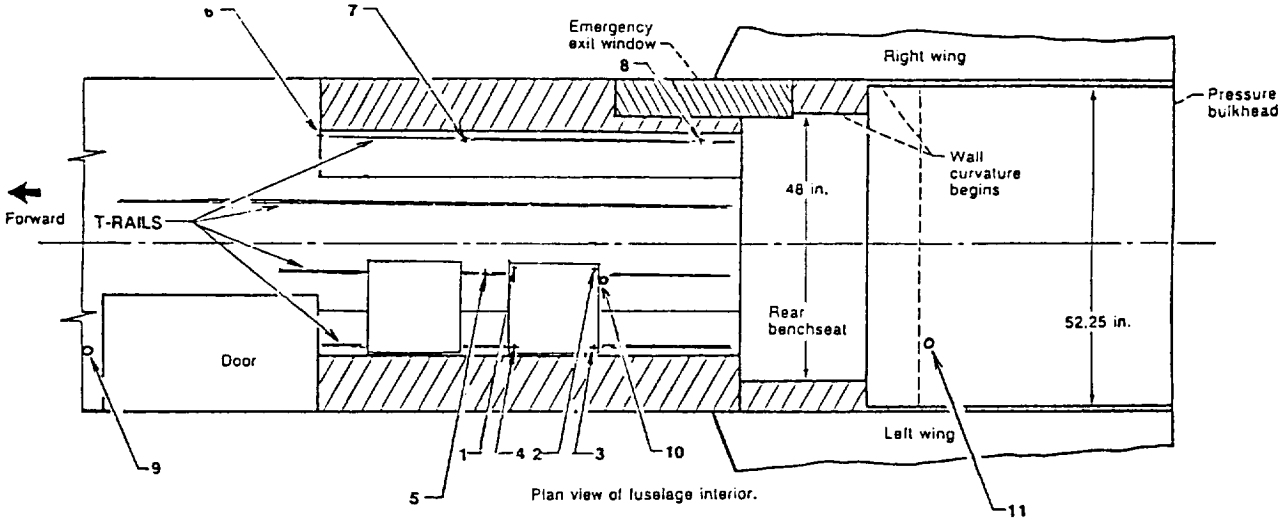

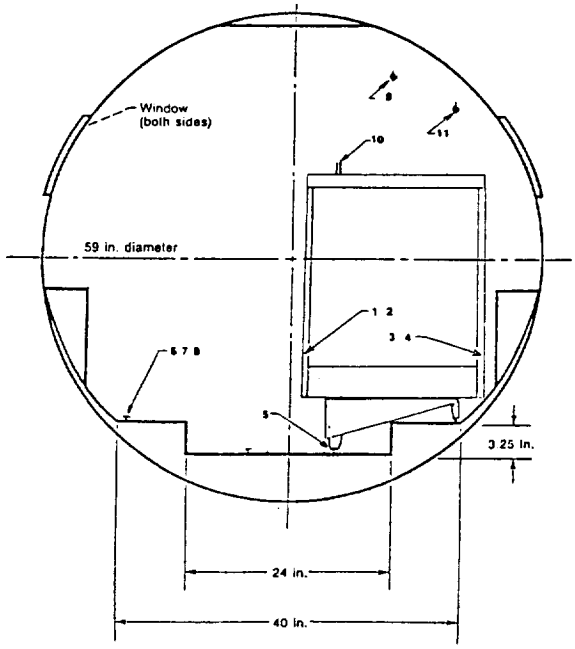

ORIGINAL PAGE IS
OF POOR QUALITY

FIGURE 3
Measurement Instrumentation Location Schematic

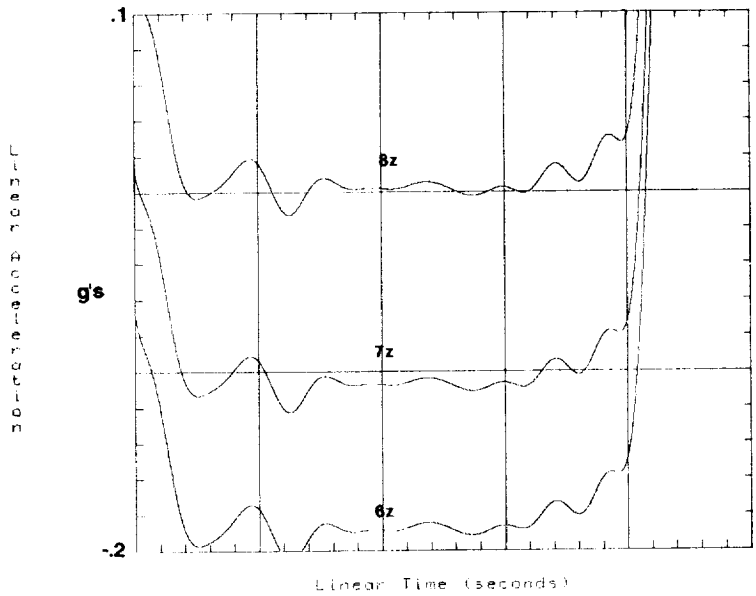

FIGURE 4

RESIDUAL ACCELERATION TREND

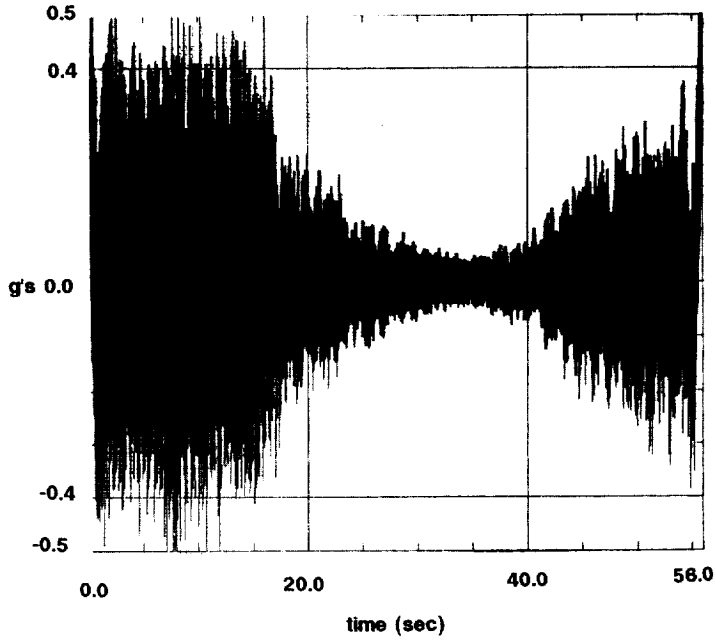

FIGURE 5
FULL TRAJECTORY HIGH FREQUENCY TIME TRACE

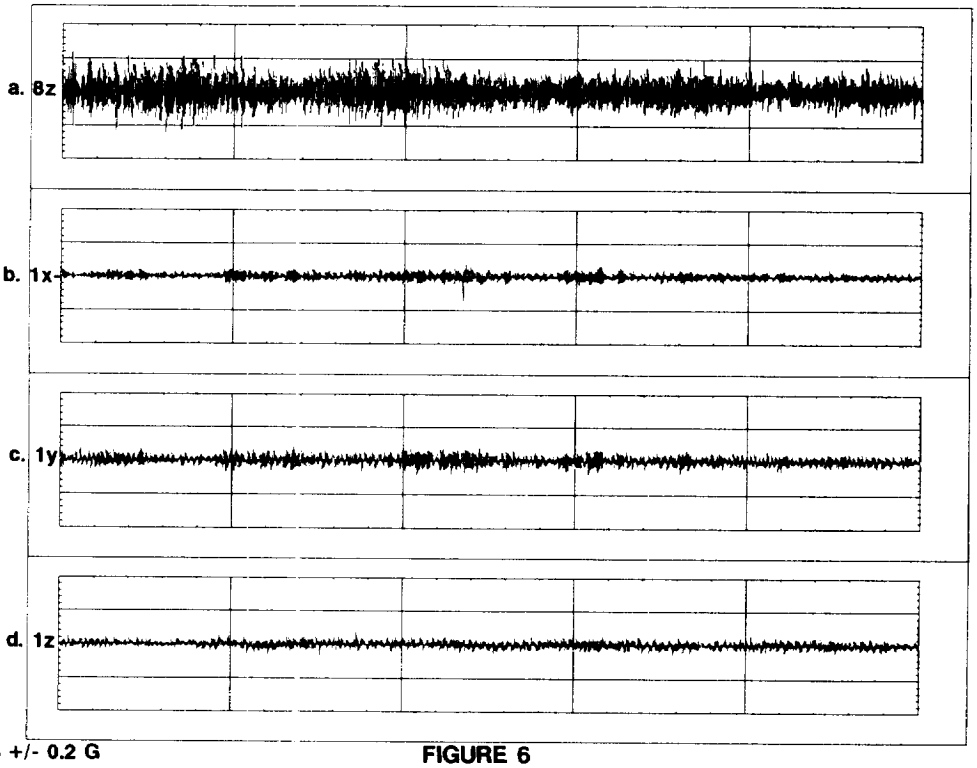

VERTICAL AXES +/- 0.2 G
5.0 SEC MICROGRAVITY

FIGURE 6
STRIPCHART VIEW

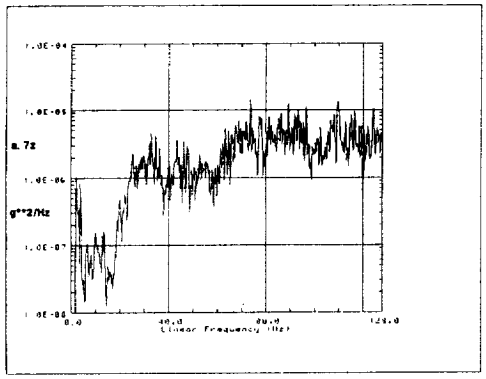

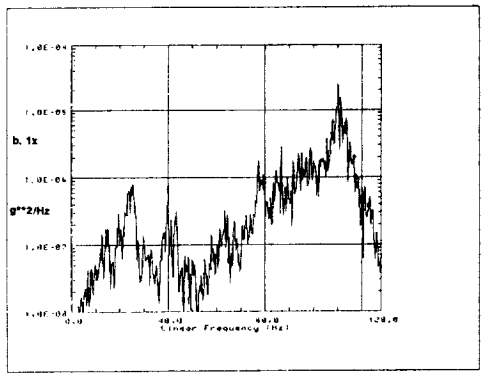

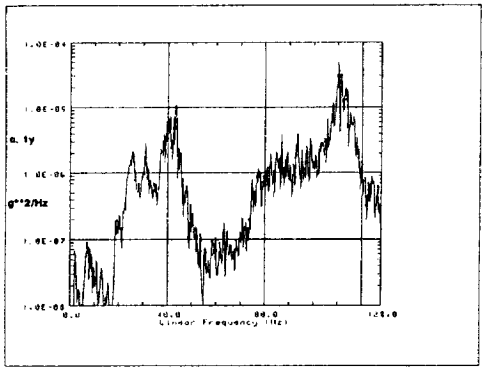

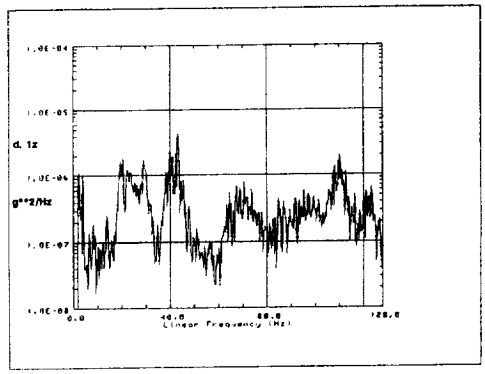

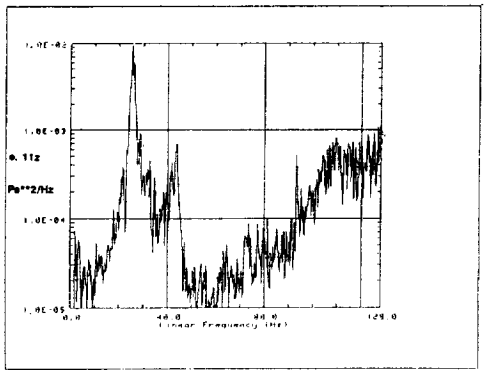

FIGURE 7

POWER SPECTRAL DENSITIES

NASA
National Aeronautics and Space Administration

Report Documentation Page

1. Report No.	2. Government Accession No.	3. Recipient's Catalog No.
NASA TM-103103		

4. Title and Subtitle

The Vibro-Acoustic Mapping of Low Gravity Trajectories on a Learjet Aircraft

5. Report Date

6. Performing Organization Code

7. Author(s)

C.M. Grodsinsky and T.J. Sutliff

8. Performing Organization Report No.

E-5427

10. Work Unit No.

694-03-03

9. Performing Organization Name and Address

National Aeronautics and Space Administration
Lewis Research Center
Cleveland, Ohio 44135-3191

11. Contract or Grant No.

13. Type of Report and Period Covered

Technical Memorandum

12. Sponsoring Agency Name and Address

National Aeronautics and Space Administration
Washington, D.C. 20546-0001

14. Sponsoring Agency Code

15. Supplementary Notes

Prepared for the Second Workshop on Microgravity Experimentation sponsored by National Research Council of Canada, Ottawa, Ontario, Canada, May 8-9, 1990.

16. Abstract

Terrestrial low gravity research techniques have been employed to gain a more thorough understanding of basic science and technology concepts. One technique frequently used involves flying parabolic trajectories aboard the NASA Lewis Research Center Learjet aircraft. A measurement program was developed to support an isolation system conceptual design. This program primarily was intended to measure time correlated high frequency accelerations (upto 100 Hz) present at various locations throughout the Learjet during a series of trajectories and flights. As suspected, the measurements obtained revealed that the environment aboard such as aircraft can not simply be described in terms of the static level low gravity "g vector" obtained, but that it also must account for both rigid body and high frequency vibro-acoustic dynamics.

17. Key Words (Suggested by Author(s))	18. Distribution Statement
Micrgravity research Ballistic trajectory Vibro-acoustic characterization Vibration isolation	Unclassified – Unlimited Subject Category 01

19. Security Classif. (of this report)	20. Security Classif. (of this page)	21. No. of pages	22. Price*
Unclassified	Unclassified	16	A03

NASA FORM 1626 OCT 86

*For sale by the National Technical Information Service, Springfield, Virginia 22161